UDC 504.062.2
IRSTI 87.35.91
DOI 10.37238/2960-1371.2960-138X.2026.103(3).30

Akhmet Ramazan*, Lyailim Taizhanova, Samal Syrlybekkyzy

Yessenov University, Caspian State University of Technologies and Engineering Named After Sh. Yessenov, Aktau, Kazakhstan
***Corresponding author:** akhmet.ramazan@yu.edu.kz

E-mail: akhmet.ramazan@yu.edu.kz, lyailim.taizhanova@yu.edu.kz, samal.syrlybekkyzy@yu.edu.kz

ENVIRONMENTAL ASSESSMENT OF LOW-CARBON SEAWATER REVERSE OSMOSIS WITH HYBRID RENEWABLES FOR WEST KAZAKHSTAN OPTIMIZATION

Annotation. Global water scarcity, exacerbated by climate change and rapid economic growth, has led to a growing reliance on seawater reverse osmosis (SWRO). While SWRO now accounts for more than 70 % of global desalination capacity, it remains an energy-intensive process that typically consumes 3–5 kWh per cubic metre. Using fossil-fuelled electricity undermines the environmental benefits of desalination and contradicts climate-change commitments. This study analyses the techno-economic and environmental performance of a low-carbon hybrid energy system for a 100 $m^3\ day^{-1}$ SWRO plant in arid western Kazakhstan. Hourly wind data and a HOMER Pro simulation are used to identify the optimal combination of three 95 kW wind turbines, a 25 kW diesel generator, a 1.2 MWh lithium-ion battery bank and a 20 kW converter. Results show that the optimized system dramatically outperforms a diesel-only baseline, reducing the net present cost from $7.11 million to $2.06 million and lowering the levelized cost of energy to 0.5907 USD kWh^{-1}. Wind energy provides 84.8 % of the annual load, cutting diesel use to 12 770 litres and lowering CO_2 emissions by around 63 $t\ yr^{-1}$. However, approximately 84 % of generated power is curtailed because the wind capacity is oversized, resulting in a high levelized cost compared with best-practice hybrid systems. The study concludes that wind-diesel-battery systems can deliver reliable, low-carbon water supply in western Kazakhstan, but that integrating photovoltaic generation, selling surplus electricity or producing green hydrogen will be essential to minimize curtailment, improve economic viability and enhance sustainability.

Keywords: Seawater reverse osmosis; Low-carbon technology; Wind battery; Levelized cost of energy; HOMER Pro; West Kazakhstan; Green hydrogen; Water–energy nexus.

Introduction

The global freshwater crisis has emerged as one of the most pressing challenges of the 21st century, with approximately four billion people experiencing severe water scarcity for at least one month per year. Climate change, population growth, rising living standards, and accelerating urbanization are placing immense strain on natural resources, resulting in an unsecured availability of water as an existential resource [1]. This challenge is particularly acute in arid and semi-arid regions where the demand for freshwater substantially exceeds the

available supply. By 2050, projections indicate that 40% of the world's population will face water stress, with demand increasing by 55%, underscoring the urgent need for sustainable alternative water sources [2]. Seawater desalination has become an increasingly viable solution for addressing freshwater scarcity, with global capacity exceeding 100 million cubic meters per day and more than 150 countries currently utilizing desalination technologies. Seawater reverse osmosis (SWRO) has emerged as the dominant technology, accounting for more than 70% of global desalination capacity due to its compatibility with renewable energy systems and relatively lower energy consumption compared to thermal processes [3]. However, desalination remains an energy-intensive practice, with modern SWRO systems consuming approximately 3–5 kWh/m³ of produced water-still considerably higher than the theoretical thermodynamic minimum of approximately 1.1 kWh/m³ at 50% recovery. When conventional grid electricity derived from fossil fuels powers these systems, the resulting carbon footprint poses significant environmental concerns that contradict global climate commitments under the Paris Agreement and the United Nations Sustainable Development Goals (SDG 6) [4,5].

Central Asia, including Kazakhstan, represents a region particularly vulnerable to water scarcity challenges due to its arid climate, uneven spatial and temporal distribution of freshwater resources, and transboundary water management complexities [6]. Kazakhstan, characterized as a semi-arid region with dry steppe land in the south, faces increasing water deficits exacerbated by climate change and agricultural irrigation demands. The western coastal regions along the Caspian Sea, notably the Mangystau region, confront acute water supply challenges that necessitate innovative solutions combining desalination with sustainable energy sources [7]. Despite significant deposits of fossil fuels, Kazakhstan has substantial renewable energy potential estimated to exceed 1,000 billion kWh/year, with particularly favorable wind resources in the Caspian, northwestern, central, and northern corridors. The juxtaposition of severe water stress and abundant renewable energy resources makes western Kazakhstan an ideal location for investigating low-carbon desalination systems powered by hybrid renewable energy configurations [7].

Literature Review

Hybrid wind-diesel-battery systems provide a low-carbon pathway for seawater desalination by reducing CO_2 emissions by 60-92% and energy costs by 43-62% while producing water at costs ranging from 0.414 to 5.38 USD per cubic meter.

Hybrid wind-diesel-battery systems for seawater desalination offer low-carbon solutions with concrete techno-economic and environmental advantages. Studies report that optimal configurations often combining wind (with or without photovoltaic components), diesel backup, and battery storage-achieve energy cost reductions of 43-62% relative to diesel-only systems [8]. Water production costs range from about 0.414 to 5.38 USD per cubic meter; larger installations (e.g., 109,500 m³/day) yield competitive rates near 0.85 USD/m³, while smaller systems tend to be more expensive [9]. Environmental assessments indicate CO_2 emissions reductions between 60% and 92% alongside renewable energy contributions of 73.7-100% [1]. Multi-objective optimization using tools such as HOMER Pro demonstrates that appropriate sizing of components and smart storage management improve reliability and reduce energy curtailment. Geographic analysis shows that Middle Eastern, Mediterranean, and Atlantic Island projects adapt designs to local resource and infrastructure constraints, confirming that hybrid approaches can significantly lower the carbon footprint of seawater desalination [10].

Table 1 - Characteristics of Included Studies

Study	Desalination Capacity (m^3/day)	Hybrid System Configuration	Assessment Focus	Location
Elmaadawy et al., 2020	1,500	Photovoltaic (PV)/wind/diesel/battery with converter	Techno-economic and environmental feasibility	Abo Ramad village, Egypt
Hamdi et al., 2025	50,000	Solar/wind with battery storage	Techno-environmental optimization and dynamic behavior	Djerba Island, Tunisia
Gökçek and Özkan, 2023	No mention found	PV/wind/diesel/battery with converter	Technical, environmental, and economic modeling	South and west coast of Turkey
Gomaa et al., 2023	12,000	PV/wind/diesel/battery	Economic and environmental analysis	Aqaba, Jordan
Caldera et al., 2017	No mention found	PV/wind with battery storage	Integrated water-energy system transition	Saudi Arabia
Hassan et al., 2024	100	Wind/diesel/battery	Optimal sizing and management	NEOM city, Saudi Arabia
Ababneh and Al-Odat, 2024	109,500	Wind/diesel/battery	Feasibility and benefits assessment	Aqaba, Jordan
Cabrera et al., 2024	No mention found	Wind/battery	Carbon footprint reduction	Canary Archipelago
Najjar et al., 2022	No mention found	Various renewable-grid combinations	Life cycle assessment and cost analysis	Multiple locations
Schär et al., 2023	No mention found	Renewable energy with storage	Optimization of sustainable desalination	No mention found

Hybrid renewable energy systems for desalination demonstrate substantial environmental and techno-economic advantages over conventional diesel-based configurations, achieving both significant emissions mitigation and considerable cost reductions across diverse system scales. Environmentally, the highest carbon-reduction performance was observed in wind/diesel/battery systems, such as the 92% CO_2 decrease reported by Ababneh and Al-Odat (2024), which also achieved an 83.6% renewable energy fraction [14]. Similarly, PV/wind/diesel/battery configurations showed an 81.5% reduction in CO_2 emissions together with a 73.7% increase in renewable penetration, confirming the environmental efficacy of mixed renewable-diesel systems [8]. Fully renewable configurations, including PV/wind/battery, reached 98-100% renewable fractions in Gomaa et al. (2023) and Caldera et al. (2017), though absolute emission values remained scale-dependent [11,12]. Techno-economically, hybrid systems consistently outperformed diesel-only baselines, with the lowest energy cost being 0.063$/kWh achieved in a PV/wind/diesel/battery system for large-scale desalination [11]. Substantial cost

improvements were also reported by Elmaadawy et al. (2020), who documented a 62% reduction in energy cost and a 60.7% decrease in net present cost relative to diesel. Additional techno-economic optimization was demonstrated by Gökçek and Özkan (2023), with an optimal cost of 0.301 $/kWh, outperforming diesel's 0.529 $/kWh, while Ababneh and Al-Odat (2024) reported competitive water production costs as low as 0.85 $/m³ for a 109,500 m³/day installation. Although fully renewable systems exhibited higher water production costs-ranging from 3.10 to 5.38 $/m³ due to storage penalties wind-dominant hybrids maintained moderate energy costs (0.337-0.564 $/kWh), demonstrating robust economic performance [13]. Collectively, these findings indicate that multi-source hybridization and proper system optimization can reduce energy costs by 43-62% while simultaneously achieving 60-92% reductions in CO_2 emissions, underscoring the strategic value of renewable-integrated desalination in sustainable water-energy systems.

The reviewed studies demonstrate a broad diversity of geographic, technological, and system-scale contexts, highlighting the global relevance of integrated desalination-hydrogen production systems across arid, coastal, and urban environments. Gigawatt-scale modeling conducted in coastal southern Europe illustrates the feasibility of coupling seawater desalination with proton exchange membrane electrolysis powered by wind and solar resources [18]. In the Arabian Peninsula, feasibility and sensitivity analyses conducted in arid coastal regions show multigeneration systems producing between 2,709 and 8.2 million kilograms of hydrogen per year through combinations of solar photovoltaics, wind energy, reverse osmosis desalination, and both fuel-cell and alkaline electrolysis technologies [19–21]. Additional modeling work in Oman and Morocco explores scales ranging from 1,500 kilograms per day to 40 tonnes per year using treated effluent-powered reverse osmosis and wave-wind hybrid systems, respectively [22,23]. Large-scale national assessments, such as those conducted for Australia, estimate hydrogen potentials nearing 0.88 million tonnes annually, underscoring resource-driven strategic opportunities [24]. Pre-feasibility analyses in South America similarly identify substantial production potential up to 1 million kilograms per year through arid-coastal solar and RO alkaline electrolysis hybrids [25]. Finally, emerging modeling evidence indicates the viability of integrating treated wastewater with membrane-based desalination and solar-driven electrolysis to support urban hydrogen production exceeding 1,900 kilograms per hour [26]. Collectively, these studies underscore a consistent pattern: arid coastal regions exhibit the strongest alignment of renewable resources, desalination demand, and hydrogen production potential, making them strategic loci for future hydrogen-water nexus development.

Materials and methods

Location and site characterization

This study focuses on an arid coastal zone in West Kazakhstan near the Caspian Sea. The chosen site is defined by geographic coordinates of latitude 44° 41′ 19.25″ N and longitude 50° 28′ 42.00″ E. The terrain is relatively flat and near sea level, with an elevation of approximately 0 m above mean sea level. The area experiences a continental desert climate characterised by hot, dry summers and cold winters. Mean annual temperature, relative humidity and precipitation are 12.33 °C, 57.2 % and 100 mm, respectively. Given that the desalination system is powered by renewable energy, a quantitative assessment of the local wind and solar resource regime was undertaken to parameterize the energy model. Hourly meteorological series-wind speed at a defined reference height, global horizontal irradiance (GHI), and ambient air temperature were compiled and processed using HOMER Pro (version 3.18.3). The datasets span at least one

full year (≥8,760 h) and were verified to reflect inter-annual variability through cross-checks against long-term site climatology. Prior to ingestion into the modelling workflow, all series were harmonized to a common timestamp (UTC+5), screened for completeness, and subjected to consistency and bias checks. These curated inputs constitute the definitive resource basis for the subsequent techno-economic and environmental simulations.

Table 2 - Climate and resource summary for the study site.

Month	Mean wind speed (m s^{-1})	GHI (kWh m^{-2} $month^{-1}$)	Ambient temperature (°C)
January	7.490	1.250	0.320
February	7.780	2.140	-0.420
March	7.460	3.440	3.120
April	7.140	4.900	10.040
May	6.240	6.220	17.170
June	6.220	6.820	23.410
July	5.700	6.730	26.420
August	5.910	5.940	25.550
September	6.630	4.660	20.020
October	7.110	2.870	13.290
November	7.320	1.510	6.650
December	7.570	1.050	2.420

Load profile and desalination unit specification

The primary load in this study is a seawater reverse osmosis (SWRO) desalination plant. Daily potable water demand for the target coastal community is 46 000 $m^3 \cdot d^{-1}$ (peaking at 70-77×10^3 $m^3 \cdot d^{-1}$ and causing deficits of 20-25×10^3 $m^3 \cdot d^{-1}$ in summer). Commercial SWRO modules are available with different permeate capacities; for instance, units rated at 24 $m^3 \cdot d^{-1}$, 120 $m^3 \cdot d^{-1}$ and 480 $m^3 \cdot d^{-1}$ can be considered. The actual operating strategy depends on the combination of unit size and desired daily output. Each module is characterised by its permeate recovery ratio, feed water total dissolved solids (TDS), product water TDS, operating pressure, and specific energy consumption (SEC). Since local seawater salinity and temperature influence SEC, a conservative SEC range of 3-15 kWh m^{-3} is adopted for placeholder purposes.

Table 3 - SWRO unit specification.

Parameter	Unit	Module 1	Module 2	Module 3
Rated permeate flow	$m^3 \cdot d^{-1}$	24	120	480
Recovery ratio	%	30	30	30
Feed water TDS	mg L^{-1}	35 000	35 000	35 000
Product water TDS	mg L^{-1}	500	500	500
Operating pressure	bar	55	55	55
Specific energy consumption	kWh m^{-3}	3	8	15

If the daily water demand Q_d exceeds the rated flow of a single module, multiple modules can operate in parallel. The hourly permeate flow rate Q_h ($m^3 \cdot h^{-1}$) required to meet daily demand is calculated as:

$$Q_h = \frac{Q_d}{24}$$

where 24 h d^{-1} is the number of hours in a day. The electrical load of the RO system at each hour is computed as:

$$P_{RO}(t) = SEC \times Q_h(t)$$

Here SEC is the specific energy consumption, and $Q_h(t)$ may vary if an intermittent operating strategy is implemented. The resulting power demand profile should be input to HOMER Pro as a primary, time-varying load. If demand side management such as water storage is planned, $P_{RO}(t)$ may be defined as a deferrable load with an assigned priority.

System description and schematic

The proposed hybrid renewable energy system combines wind turbines (WT), photovoltaic (PV) modules (if included), a diesel generator (DG), battery storage (BS), a power electronics converter (inverter/rectifier), and the SWRO load. The DC bus connects the wind turbines, battery and PV subsystems via rectifiers, while the AC bus supplies the SWRO plant and other auxiliary loads. The control system manages power dispatch among components according to predefined strategies

Table 4 - Component nomenclature

Component	Symbol	Unit	Design parameter	Typical range
Number of wind turbines	N_{WT}	-	integer	1-10
Rated power of one wind turbine	$P_{WT,r}$	kW	1500	500-2000
PV array rated power	$P_{PV,r}$	kW	1000	0-2000
Diesel generator rated power	$P_{DG,r}$	kW	500	0-500
Battery bank capacity	C_B	kWh	3000	0-5000
Converter capacity	P_{Conv}	kW	1000	0-2000
Rated SWRO load	$P_{RO,r}$	kW	3000	2000-5000

During operation, the instantaneous power balance at any time t must satisfy:

$$P_{WT}(t) + P_{PV}(t) + P_{DG}(t) = P_{RO}(t) + P_{loss}(t) + P_{charge}(t) - P_{discharge}(t)$$

where P_{loss} represents conversion losses, P_{charge} is battery charging power, and $P_{discharge}$ is battery discharge power.

Wind turbine modelling

Wind speed at hub height is estimated from the measured wind speed at reference height using the power law [Hassan et al. 2024]:

$$V_{hub}(t) = V_{ref}(t)\left(\frac{H_{hub}}{H_{ref}}\right)^{\alpha}$$

where $V_{ref}(t)$ is the reference wind speed at height H_{ref}, $V_{hub}(t)$ is the wind speed at hub height H_{hub}}, and α is the surface roughness exponent. For this study, the hub height and reference height are set to 80 m and 50 m, respectively, consistent with the meteorological dataset.

The power output of a wind turbine with rated power $P_{WT,r}$ follows a piecewise function depending on the hub wind speed $V_{hub}(t)$:

$$P_{WT}(t) = \{0, V_{hub}(t) < V_{ci}\ P_{WT,r}\frac{V_{hub}(t)^3 - V_{ci}^3}{V_r^3 - V_{ci}^3},$$

$$V_{ci} \le V_{hub}(t) < V_r\ P_{WT,r}, V_r \le V_{hub}(t) \le V_{co}\ 0, V_{hub}(t) > V_{co}$$

where V_{ci}, V_r and V_{co} are the cut-in, rated and cut-out wind speeds, respectively.

If multiple turbines are installed, the total wind power is $P_{WT,tot}(t) = N_{WT}$ times $P_{WT}(t)$. Loss factors such as blade aerodynamic efficiency, gearbox and generator efficiency,

and array losses can be applied via an overall wind turbine efficiency $\eta_{WT} = 0.38$. The annual energy generated by wind turbines is:

$$E_{\mathrm{WT,ann}} = \sum_{t=1}^{8760} P_{\mathrm{WT,tot}}\,(t)\Delta t$$

where Δt is the simulation time step (s or h). Air density corrections may be implemented based on site temperature and pressure [27].

Diesel generator modelling

The diesel generator supplies power when renewable generation and stored energy are insufficient. The fuel consumption F (L h^{-1}) of a generator operating at output $P_{DG}(t)$ is commonly expressed as a linear function:

$$F(t) = a_1 P_{DG}(t) + a_2 P_{DG,r}$$

where $P_{DG,r}$ is the rated capacity of the generator, and a_1 and a_2 are coefficients representing fuel consumption per unit power and idling consumption, respectively).

The generator output at each hour is limited to:

$$0 \le P_{DG}(t) \le P_{DG,r}$$

Engine start-up and minimum load constraints may be defined according to manufacturer specifications. The net present cost (NPC) of the diesel generator over project lifetime N years is computed as:

$$\mathrm{NPC_{DG}} = C_{\mathrm{cap,DG}} + \sum_{y=1}^{N} \frac{C_{\mathrm{O\&M,DG}}(y) + C_{\mathrm{fuel,DG}}(y) + C_{\mathrm{rep,DG}}(y)}{(1+i)^y} - S_{\mathrm{DG}}$$

where $C_{cap,DG}$ is the capital cost, $C_{O\&M,DG}(y)$ is the annual operation and maintenance cost, $C_{fuel,DG}(y)$ is the annual fuel cost (based on diesel fuel price of 0.8 USD L^{-1}*[1]* and consumption F(t)), $C_{rep,DG}(y)$ is the replacement cost when the generator reaches its lifetime (in hours), i is the discount rate, and S_{DG} is the salvage value at the end of life. Emission analysis may be included by multiplying annual fuel consumption by a diesel emission factor.

Battery storage modelling

Battery storage moderates the variability of wind generation and reduces diesel operation. Let C_B (kWh) denote the nominal energy capacity of the battery bank. The battery state of charge (SOC) at time step t is updated by integrating the battery power:

$$SOC(t) = SOC(t-1) + \frac{\eta_{ch} P_{charge}(t) - \frac{P_{discharge}(t)}{\eta_{dis}}}{C_B}$$

where η_{ch} and η_{dis} are the charge and discharge efficiencies, respectively.

The SOC is constrained between a minimum allowable depth of discharge (DOD) and 100 %. The battery cannot charge and discharge simultaneously.

For preliminary sizing, the required battery capacity C_B (kWh) to support the load during an autonomy period of T_{aut} days can be estimated by:

$$C_B = \frac{P_{load,avg} \times T_{aut} \times 24}{\eta_B \times \eta_{conv} \times (1 - DOD)}$$

where $P_{load,avg}$ (kW) is the average load (here equal to $P_{RO}(t)$ if other loads are negligible), η_B is the round-trip battery efficiency, η_{conv} is the converter efficiency, and DOD_{min} is the maximum depth of discharge permitted. Battery lifetime is specified either in years or number

of cycles at a given DOD. Cycle counting methods (rainflow algorithm) may be applied to estimate degradation [27].

Control and Energy Management Strategies

Energy management governs the dispatch sequence of sources to meet the load while minimising cost and fuel consumption. The three strategies considered are load following, cycle charging, and combined dispatch, as in Hassan et al [27].

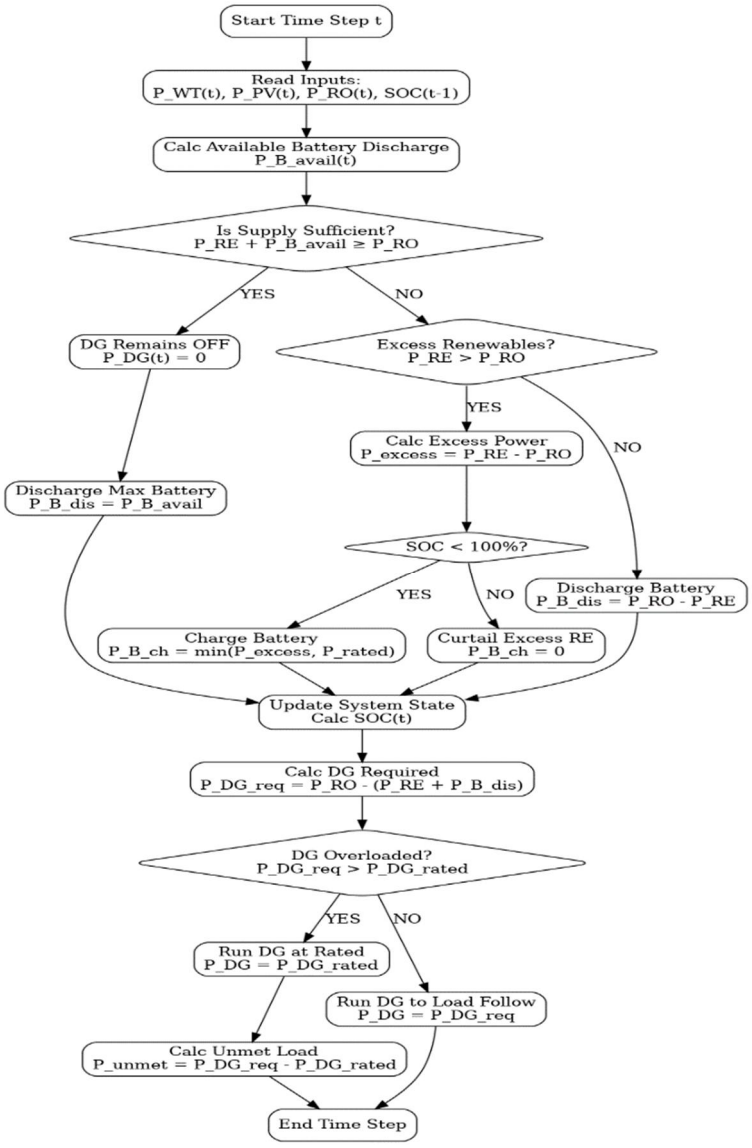


Figure -1 Cycle Charging (CC)

In Cycle Charging dispatch, once the DG is started, it operates at rated capacity regardless of instantaneous load (Figure -1). The surplus power charges the battery until it reaches the upper SOC setpoint. The DG then switches off, and the load is met by renewable generation and battery discharge until SOC falls to the lower setpoint (Figure -2).

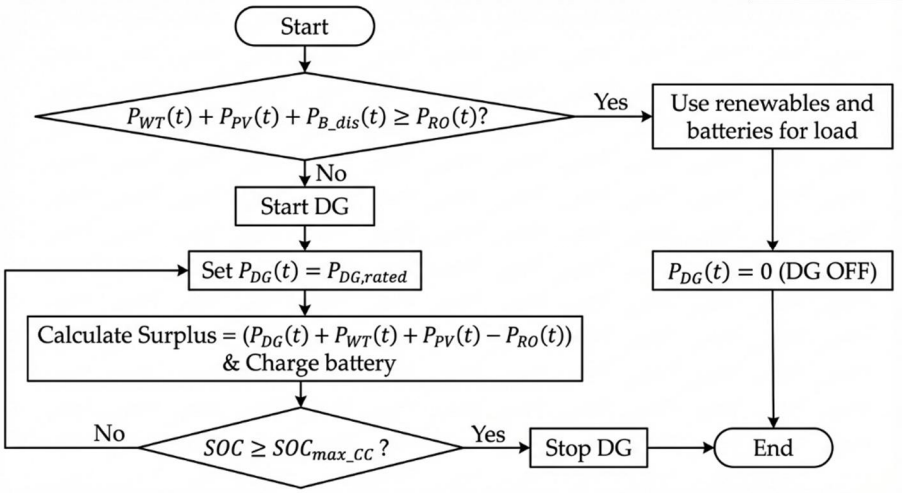


Figure - 2 SOC thresholds and battery setpoints for starting/stopping the DG should be defined.

The combined strategy is a hybrid of LF and CC. It uses LF as default but invokes CC when battery SOC drops below a critical threshold to prevent deep discharge.

Evaluation metrics and economic model

Technical and economic performance indicators are calculated to compare system configurations. The total net present cost (NPC) of the hybrid system is the sum of NPC contributions from all components:

$$\mathrm{NPC_{tot}} = \sum_j \mathrm{NPC}_j$$

where j indexes components: wind turbines, PV, diesel generator, battery, converter, and SWRO plant. NPC is calculated from annualised cost using the capital recovery factor (CRF):

$$NPC_j = \frac{C_{ann,j}}{CRF(i,N)}$$

$$CRF(i,N) = \frac{i(1+i)^N}{(1+i)^N - 1}$$

where $C_{ann,j}$ is the total annualised cost of component j, i is the real discount rate, and N is the project lifetime in years. Salvage value at the end of life is computed as:

$$S_j = C_{cap,j} \times \left(1 - \frac{t_{op}}{L_j}\right)$$

where $C_{cap,j}$ is the capital cost, t_{op} is the project duration, and L_j is the component lifetime. Components replaced during the project have their own salvage values.

The levelised cost of energy (LCOE) or cost of energy (COE) is the ratio of total annualised cost to total energy supplied to the load:

$$\mathrm{COE} = \frac{\sum_j C_{\mathrm{ann},j}}{\sum_{t=1}^{8760} P_{\mathrm{load}}(t)\Delta t}$$

For the desalination context, a levelised cost of water (LCOW) may be estimated by dividing the total annual cost (including O&M for membranes, chemicals, labour) by the annual water production:

$$LCOW = \frac{C_{ann,tot}}{Q_{ann}}$$

where Q_{ann} is the annual permeate volume (m^3). Financial indicators such as internal rate of return (IRR), net present value (NPV), and simple payback period are computed using standard cash-flow analysis [27].

System reliability is assessed via the renewable fraction f_{ren} calculated as

$$f_{ren} = 1 - \frac{E_{DG}}{E_{load}}$$

where E_{DGE} denotes the diesel generator output (kWh), and E_{load} is the total load demand (kWh).

Complementary performance metrics included the unmet load ratio (ULR), excess renewable energy ratio (ERER), and battery throughput (BT), which respectively describe system deficiency, renewable energy oversupply, and storage utilization.

To evaluate the robustness of the design, sensitivity analyses will be performed by varying key parameters within plausible ranges. For each parameter, a baseline value and a set of alternative values are defined:

- Wind resource scaling factor**:** 0.9-1.1
- Diesel fuel price**:** 0.8-1.2 USD L^{-1}
- Discount rate**:** 10-20 %
- Battery cost per unit capacity**:** 250-400 USD kWh^{-1}
- Specific energy consumption of SWRO**:** 3-15 kWh m^{-3}
- Projected water demand**:** 46 000 m^3 d^{-1} ± 20 %
- Battery depth-of-discharge setpoint**:** 70-90 %

Each parameter will be varied one-at-a-time while keeping others constant to generate a tornado chart illustrating sensitivity of NPC and COE. Additionally, scenario analyses will compare different system architectures (e.g., with and without PV, alternative SWRO unit sizes) and dispatch strategies. Step sizes for parameter variation and number of scenarios should be defined.

Results

The optimal system configuration identified in HOMER Pro comprises three EXO-M-26 wind turbines (95 kW each, totaling 285 kW), a diesel generator sized to match the SWRO_100 m³/day desalination load (nominally 25 kW), a 20-kW bidirectional converter, and a battery bank of 12 × 100 kWh (nominal capacity 1,200 kWh; usable capacity 960 kWh). For this architecture, the total net present cost (NPC) amounted to $2.06 million, the levelized cost of energy (LCOE) was $0.5907/kWh, and the annual operating expenses were $82.4 thousand per year, with initial capital expenditures of $746.6 thousand. For the baseline (diesel-dominated) solution, the indicators are less favorable: NPC = $7.11 million, LCOE = $2.04/kWh, and O&M costs = $423 thousand per year. The economic comparison shows an internal rate of return (IRR) of 81.5%, a return on investment (ROI) of 89.1%, and a simple payback period of 1.38 years (discounted payback: 1.42 years). As shown in Figure 3 and Table 5, the optimized hybrid system dramatically reduces NPC and LCOE relative to the diesel base, while improving payback and profitability.

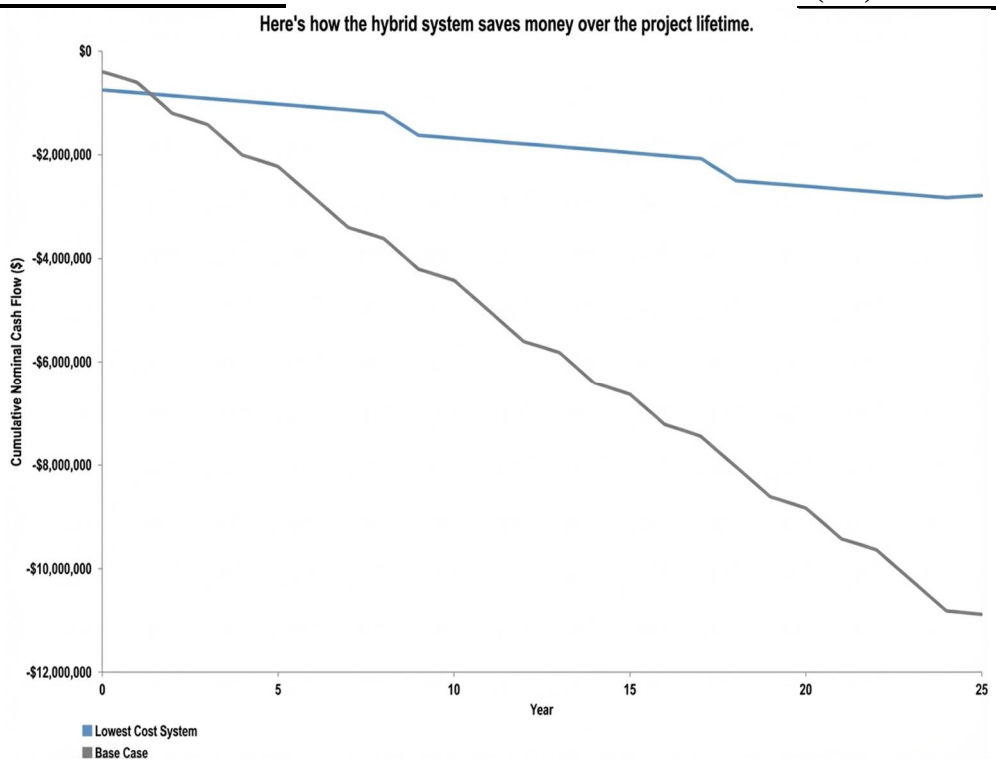


Figure 3 - Summary project economics and cumulative cash flow: baseline vs. optimized WT-DG-BESS system.

Table 5 - Economic and operational comparison of the baseline and optimized configurations

Metric	**Base case (Diesel-only)**	**Optimized hybrid (3 WT + DG + Li-ion)**
NPC (Net Present Cost), $	7,110,000	2,057,326
LCOE, $/kWh	2.04	0.5907
Operating cost, $/yr	423,086	82,424
CAPEX, $	382,860	746,580
Wind turbines (XANT24 95 kW)	0	3 × 95 kW
Diesel generator (kW)	25	25
Battery capacity	0.4 MWh (4×100 kWh)	1.2 MWh (12×100 kWh)
Annual load served, kWh/yr	219,000	219,000
Excess electricity, kWh/yr	0	1,157,954
Renewable fraction, %	0	84.8
Wind energy production, kWh/yr	0	1,343,606
Diesel energy production, kWh/yr	219,000	33,348
Diesel fuel consumption, L/yr	71,613	12,770
IRR, %	-	81.5
ROI, %	-	89.1
Simple payback, yr	-	1.38

A breakdown of the NPC by component shows that the desalination unit (SWRO_100m3d) accounts for the largest share of the life-cycle cost: approximately $1.49 million (≈72%). The EXO-M-26 wind farm represents about $0.55 million (≈27%), while the

converter and battery system together contribute less than 1%. The cost structure reflects the high expenses associated with operating and periodically replacing desalination subsystem components, whereas the wind turbines deliver substantial energy generation with moderate O&M requirements. This cost structure is illustrated in Figure 4, which shows the NPC breakdown by component.

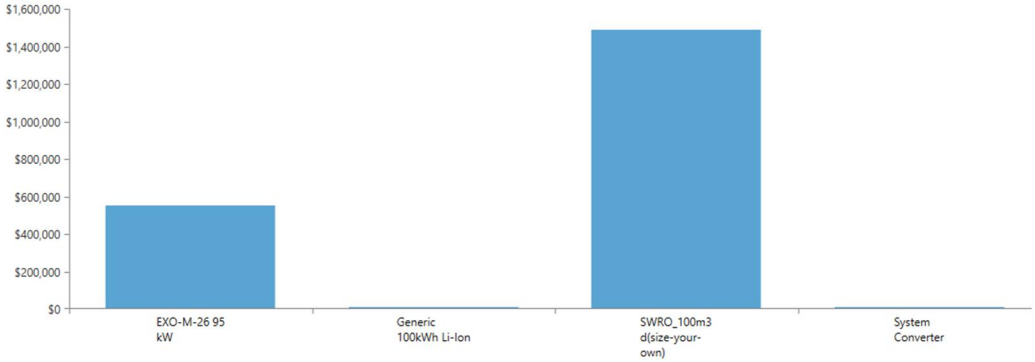


Figure 4 - Breakdown of net present cost (NPC) by system components.

The annual energy balance demonstrates a strong predominance of wind generation: total production reached 1,376,954 kWh/year, of which the EXO-M-26 turbines supplied 1,343,606 kWh/year (97.6%), while the diesel generator (SWRO_100m3d element) contributed 33,348 kWh/year (2.42%). The annual load consumption amounted to 219,000 kWh/year; due to the large installed wind capacity, a substantial energy surplus of 1,157,954 kWh/year (84.1% of total generation) was produced. The renewable fraction with respect to the load is 84.8%, and the instantaneous maximum renewable share reaches 1,080%, indicating frequent periods of overgeneration.The monthly generation profile and excess-energy output are presented in Figure 5.

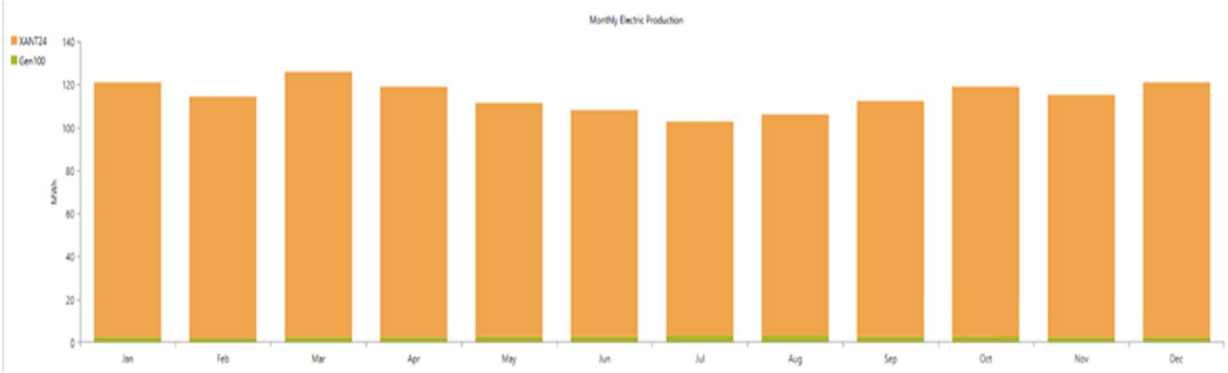


Figure 5 - Monthly generation profile: wind production, diesel contribution, and excess energy.

The monthly daily profiles of the renewable share show a daytime rise in wind penetration toward the midday and afternoon hours, followed by a decline during the night. In the windier months (autumn-winter), the penetration peak reaches 700-900% or higher, which is consistent with the corresponding diurnal wind-speed patterns. Figure 6 depicts the daily profiles of renewable-generation share by month.



Figure 6 - Daily profiles of renewable-generation share by month (Renewable Penetration).

The wind resource is characterized by stable average speeds of about 6-9 m/s during daytime hours, with an increase in the colder season. The monthly distributions (box plots) indicate frequent episodes of wind speeds exceeding 10 m/s, which explains the high annual output of the wind farm. Figures 7 and 8 illustrate the daily hub-height wind-speed profiles and the monthly wind-speed distributions (box plots), respectively.

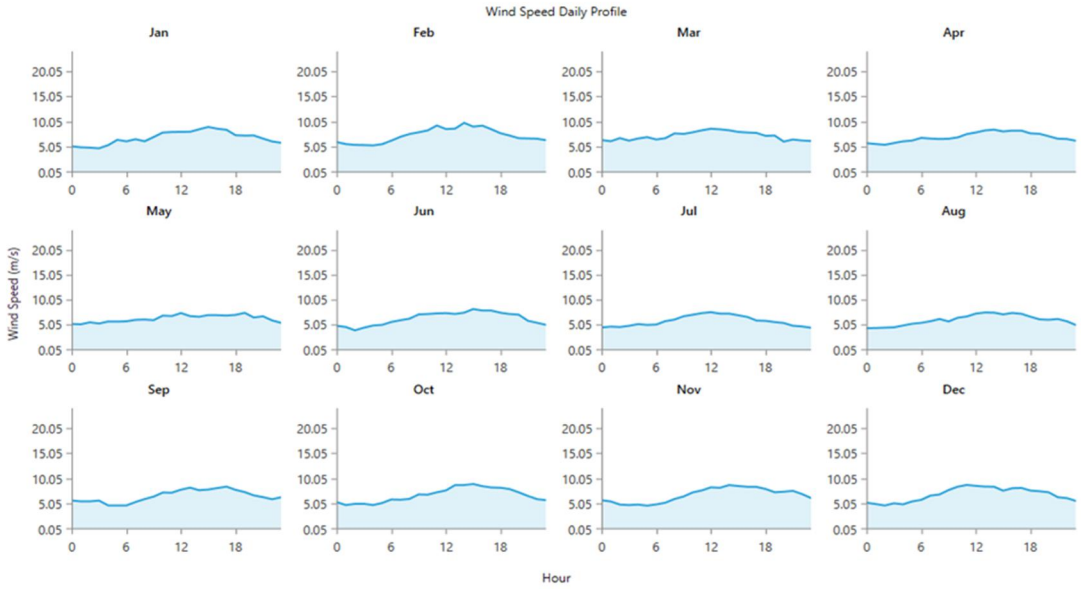


Figure 7 - Hub-height wind speed: daily profiles by month.



Figure 8 - Monthly wind-speed distributions (box plots).

The alignment between the resource and the total renewable capacity is further evident from the daily profiles of aggregate renewable power: from spring through autumn, smooth “bell-shaped” curves with afternoon peaks are observed, while in the winter months the peaks become higher and broader. This relationship is shown in Figure 9, which provides the daily profiles of total renewable power by month.

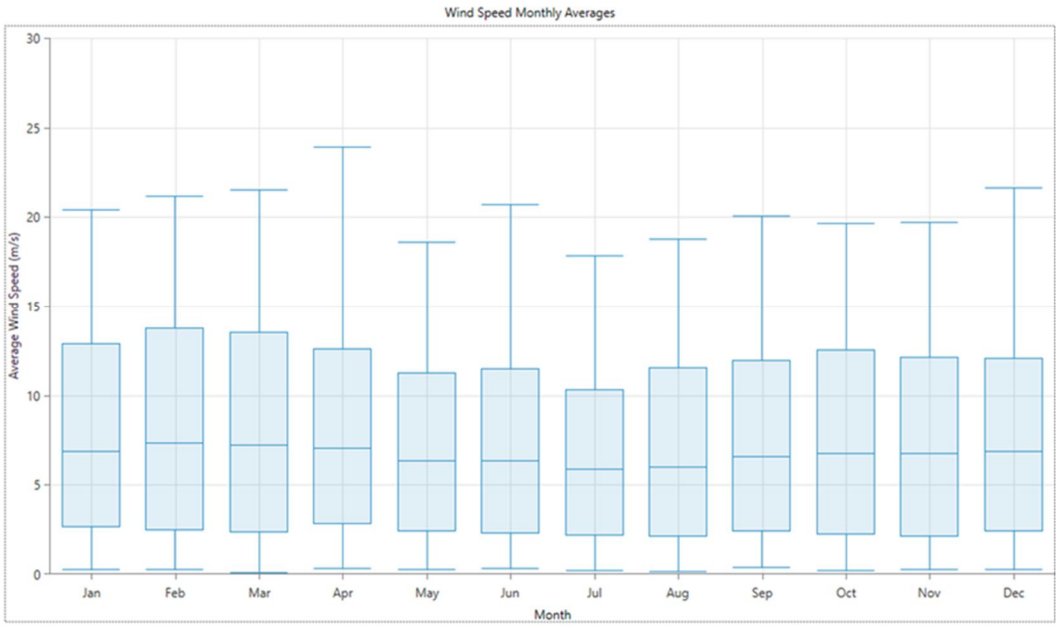


Figure 9 - Total renewable power: daily profiles by month.

The role of the diesel generator is limited to covering wind-generation shortfalls and meeting technological constraints: annual fuel consumption amounted to 12,770 liters (an average of 35.0 L/day or 1.46 L/h), with a specific fuel consumption of 0.383 L/kWh and an average electrical efficiency of 26.5%. The generator operated for 1,761 hours per year with

a capacity factor of 15.2%, delivering an average electrical output of 18.9 kW (minimum/maximum: 7.5/25 kW).Seasonal variability of diesel fuel consumption is shown in Figure 10, whereas Figure 11 provides an hourly heat map of the generator's power output.

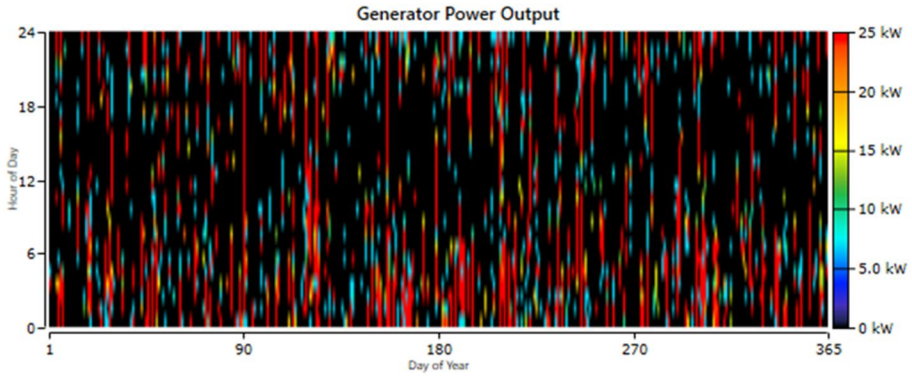


Figure 10 - Diesel fuel consumption: seasonality and variability.

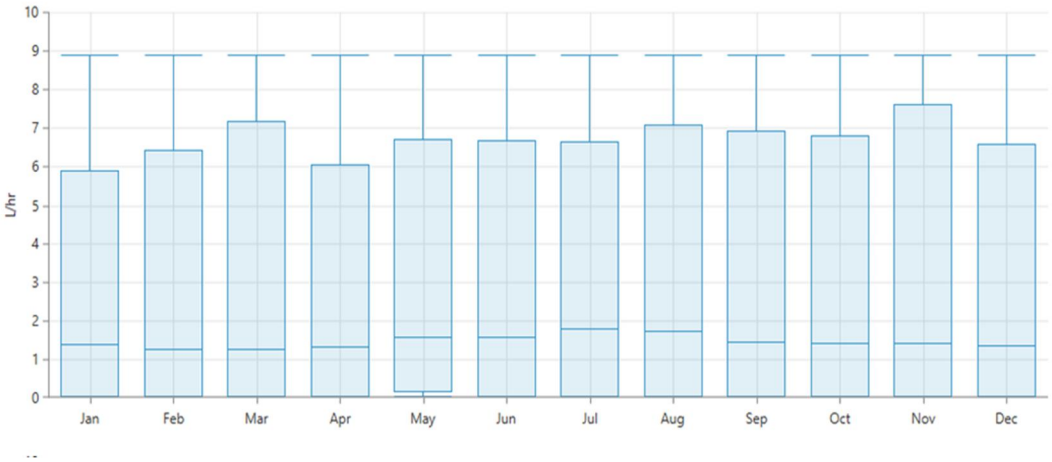


Figure 11 - Diesel-generator power output: hourly heat map over the year.

The behavior of the storage system confirms that the battery in the current configuration primarily provides smoothing and backup functions: with a nominal capacity of 1,200 kWh and a usable capacity of 960 kWh, the calculated autonomy under the baseline load reaches approximately 38.4 hours. The annual SOC profile is nearly flat (~99-100%), indicating an extremely shallow cycling depth. This is reflected in Figure 12, which presents the annual state-of-charge profile of the battery.

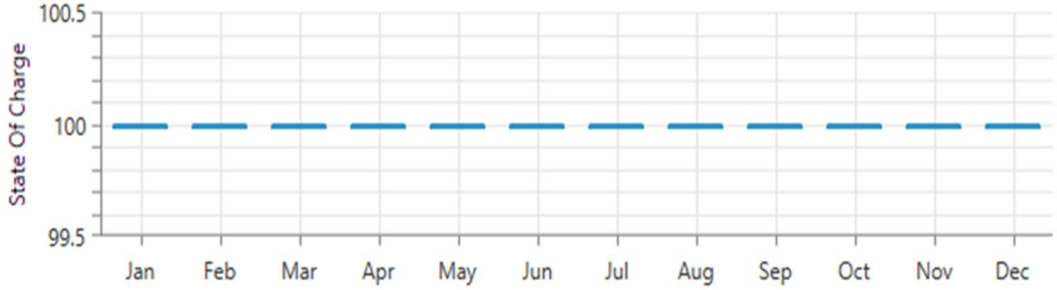


Figure 12 - Battery state of charge (SOC): annual profile.

The project's cash flows are typical for wind-diesel desalination systems: a substantial upfront investment (wind farm, battery storage, converter, and site preparation) followed by steady annual O&M expenditures. Superimposed on this pattern are the "steps" associated with major replacement and maintenance campaigns for the desalination equipment (approximately in years 9 and 18), which are partially offset by the salvage value at the 25-year horizon. Comparison with the baseline scenario shows a rapid return on investment driven by reductions in both O&M costs and fuel consumption. Figure 13 illustrates the cash flows by cost categories over the 25-year project horizon.

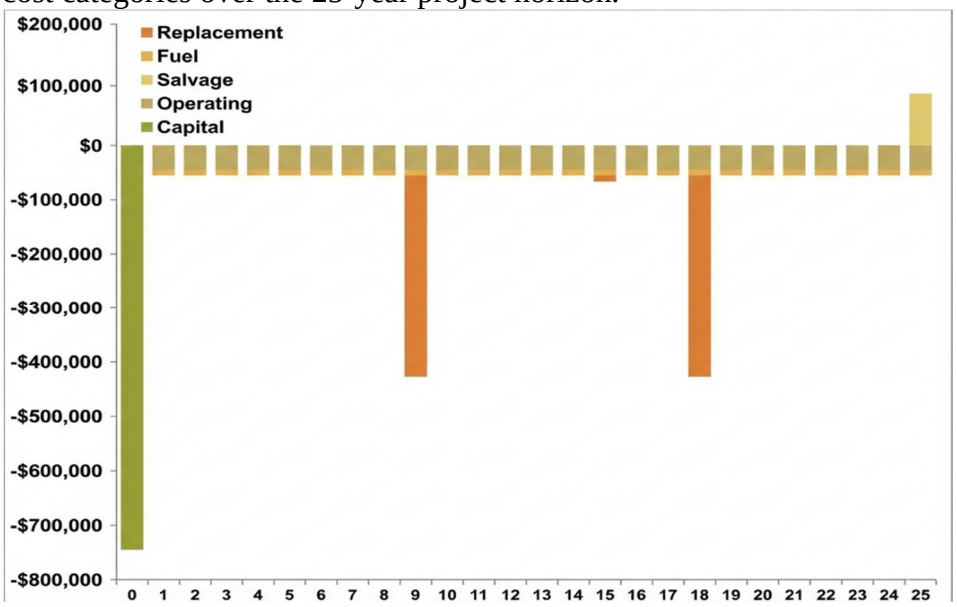


Figure 13 - Cash flows by cost categories over the 25-year horizon.

The optimized configuration achieves a dramatic reduction in NPC and LCOE relative to the diesel-based baseline while maintaining a high level of reliability (no power deficits). However, this comes with a pronounced surplus of wind generation (≈84% of total production is curtailed) and minimal utilization of the battery. This situation opens two possible directions for further development:

(i) prioritizing the integration of additional consumers (e.g., distributed loads, hydrogen production/electrolysis), thereby monetizing the surplus energy;

(ii) carefully reducing the installed wind capacity or revisiting the control strategy if the objective is to minimize capital expenditures without compromising reliability.

Discussion

This study shows that even a small SWRO plant (100 $m^3\ day^{-1}$; 219 MWh yr^{-1} demand) can operate autonomously with a wind-dominated low-carbon hybrid system while reducing costs relative to diesel-only supply. The optimal HOMER Pro configuration includes three 95 kW wind turbines, a 25 kW diesel generator, a 1.2 MWh Li-ion battery (960 kWh usable), and a 20 kW converter. The system meets the full load with minimal diesel support: annual fuel use is 12,770 L, renewable share reaches 84.8%, and LCOE and NPC are 0.5907 USD kWh^{-1} and 2.06 MUSD, respectively. However, 84.1% of generated energy is curtailed (1.16 GWh yr^{-1}), indicating severe overcapacity. Although cheaper than the diesel alternative, the LCOE remains higher than typical hybrid benchmarks and reflects underutilization of installed wind capacity. Curtailment suggests opportunities to increase desalination output, export surplus electricity, or reduce generation capacity.

Comparison with Hassan et al. (NEOM case) highlights key differences. Their optimal configuration (single 90 kW wind turbine, 25 kW diesel generator, battery bank, combined dispatch) achieved 0.337 USD kWh^{-1} LCOE and ~0.95 MUSD NPC, despite higher fuel use (36,396 L yr^{-1}). Our system shows lower diesel consumption and higher renewable share but higher LCOE due to stricter financial assumptions (16.5% discount, 12.2% inflation), load-following dispatch, and oversizing of wind generation. Curtailment below 1% in NEOM versus 84% here further confirms mismatched capacity sizing. The larger battery and turbine investment explains the doubled NPC.

Environmentally, reduced diesel use provides a clear benefit: applying an emission factor of 2.68 kg CO_2 L^{-1}, the ~65% fuel reduction lowers emissions by about 63 t CO_2 annually. Thus, the design improves carbon performance despite economic penalties. The central trade-off arises from excessive renewable surplus: low operating costs coexist with high LCOE because capital-intensive assets remain underutilized. Engineering responses include scaling production, exporting electricity, or downsizing generation. Literature indicates optimized hybrid systems typically achieve 0.301–0.377 USD kWh^{-1} and up to 0.564 USD kWh^{-1} in less efficient cases. Reported values include 0.301 USD kWh^{-1} in Turkey (PV–wind–diesel hybrid), 0.308 USD kWh^{-1} in Jordan (83.6% renewable share), and lower water production costs in Tunisia. These comparisons confirm that our 0.59 USD kWh^{-1} lies above typical ranges due to excess installed wind power (1.38 GWh generation versus 0.219 GWh load), financial assumptions, and lack of complementary sources such as PV. Published sizing guidelines reinforce this interpretation: small systems (65–100 m^3 day^{-1}) usually employ only 6–10 kW wind, 12.5–15 kW PV, and modest storage, yielding 0.166–0.280 USD kWh^{-1}, whereas medium systems resemble NEOM-scale layouts with 0.337–0.377 USD kWh^{-1}. In contrast, the present configuration deploys disproportionate wind capacity for a ~25 kW load, leading to curtailment and inefficient storage utilization. The battery barely cycles, remaining near full charge with negligible throughput, indicating excess capital allocation. Oversizing is further amplified by adopting upper-bound RO energy consumption assumptions (8–10 kWh m^{-3}) and fixed scheduling.

Overall, western Kazakhstan demonstrates strong wind potential but challenges in system integration. Elevated LCOE results from aggressive economic parameters, oversized generation and storage, and unused surplus energy. Improved sizing, flexible dispatch strategies, or diversified generation portfolios are necessary to reconcile environmental benefits with economic competitiveness.

Future work

Future work will focus on integrated techno economic modelling of the electricity to hydrogen chain including CAPEX OPEX and NPV assessment and evaluation of electrolyser operation under variable wind profiles and partial loads. A two stage optimisation will be implemented to define the minimum surplus reserved for hydrogen production and constraints on grid export. The extended model will incorporate battery degradation temperature dependent RO specific energy consumption and dynamic price scenarios. A formal comparison of three regimes - stand alone without monetisation stand alone with hydrogen production and grid connected operation - will be conducted to identify the configuration that minimises water LCOE under given risk constraints.

Conclusion

The modelling of a hybrid wind-diesel-battery system for a 100 m^3 day^{-1} seawater reverse-osmosis plant in western Kazakhstan shows that low-carbon desalination is technically feasible and economically attractive. The optimal configuration—three 95 kW

wind turbines, a 25 kW diesel generator, a 1.2 MWh battery bank and a 20 kW bidirectional converter—delivers uninterrupted power, achieves a renewable fraction of 84.8 % and cuts diesel fuel consumption to 12 770 L yr^{-1}. Compared with a diesel-only baseline, the system reduces the net present cost by 71 % and achieves a levelized cost of 0.59 USD kWh^{-1}, with an attractive payback period of about 1.4 years. Nevertheless, almost nine-tenths of the generated wind energy is curtailed due to oversized capacity, resulting in a higher energy cost than reported in comparable studies. To enhance economic and environmental performance, future work should focus on optimizing the sizing of wind turbines, incorporating photovoltaic modules, and adopting combined dispatch strategies to reduce curtailment. Monetizing surplus energy through grid export or on-site green-hydrogen production could further lower the levelized cost and enhance sustainability. Despite the oversizing challenge, the research underscores the potential of hybrid renewable-based desalination to provide reliable drinking water while reducing carbon emissions in arid coastal regions.

Acknowledgments

This research was funded by the Committee of Science of the Ministry of Science and Higher Education of the Republic of Kazakhstan (Grant No. BR24992964).

REFERENCES

[1] Lecturer in Chemistry, S.V.R.M College, Nagaram., P. Babu Racheeti, WATER CRISIS ESCALATION: GLOBAL CHALLENGES AND URGENT IMPERATIVES-REVIEW, IJAR 12 (2024) 703–710. https://doi.org/10.21474/IJAR01/18348.

[2] M.M. Mekonnen, A.Y. Hoekstra, Four billion people facing severe water scarcity, Sci. Adv. 2 (2016) e1500323. https://doi.org/10.1126/sciadv.1500323.

[3] A. Politano, R.A. Al-Juboori, S. Alnajdi, A. Alsaati, A. Athanassiou, M. Bar-Sadan, A.N. Beni, D. Campi, A. Cupolillo, G. D'Olimpio, G. D'Andrea, H. Estay, D. Fragouli, L. Gurreri, N. Ghaffour, J. Gilron, N. Hilal, J. Occhiuzzi, M.R. Carvajal, A. Ronen, S. Santoro, M. Tedesco, R.A. Tufa, M. Ulbricht, D.M. Warsinger, D. Xevgenos, G. Zaragoza, Y.-W. Zhang, M. Zhou, E. Curcio, 2024 roadmap on membrane desalination technology at the water-energy nexus, J. Phys. Energy 6 (2024) 021502. https://doi.org/10.1088/2515-7655/ad2cf2.

[4] S.G. Salinas-Rodríguez, J.C. Schippers, G.L. Amy, I.S. Kim, M.D. Kennedy, Seawater Reverse Osmosis Desalination: Assessment and Pre-treatment of Fouling and Scaling, IWA Publishing, 2021. https://doi.org/10.2166/9781780409863.

[5] A. Pistocchi, T. Bleninger, C. Breyer, U. Caldera, C. Dorati, D. Ganora, M.M. Millán, C. Paton, D. Poullis, F.S. Herrero, M. Sapiano, R. Semiat, C. Sommariva, S. Yuece, G. Zaragoza, Can seawater desalination be a win-win fix to our water cycle?, Water Research 182 (2020) 115906. https://doi.org/10.1016/j.watres.2020.115906.

[6] A. Arifjanov, L. Samiev, S. Jalilov, Overview of Sustainable Drip Irrigation Systems in Central Asia, E3S Web Conf. 574 (2024) 05004. https://doi.org/10.1051/e3sconf/202457405004.

[7] X. Jianzhong, A. Assenova, V. Erokhin, Renewable Energy and Sustainable Development in a Resource-Abundant Country: Challenges of Wind Power Generation in Kazakhstan, Sustainability 10 (2018) 3315. https://doi.org/10.3390/su10093315.

[8] K. Elmaadawy, K.M. Kotb, M.R. Elkadeem, S.W. Sharshir, A. Dán, A. Moawad, B. Liu, Optimal sizing and techno-enviro-economic feasibility assessment of large-scale reverse osmosis desalination powered with hybrid renewable energy sources, Energy

Conversion and Management 224 (2020) 113377. https://doi.org/10.1016/j.enconman.2020.113377.

[9] M. Hamdi, O. Gtari, M. Hazami, Techno-environmental optimal sizing and dynamic behavior of a hybrid system feeding a large-scale SWRO desalination system: The case of Djerba Island, Tunisia, Energy Exploration & Exploitation 43 (2025) 378–409. https://doi.org/10.1177/01445987241285463.

[10] M. Gökçek, F. Özkan, Techno-enviro-economic design of small-scale membrane-based seawater desalination systems integrated with hybrid autonomous renewable power systems, Env Prog and Sustain Energy 43 (2024) e14206. https://doi.org/10.1002/ep.14206.

[11] M.R. Gomaa, A.K. Al-Bawwat, M. Al-Dhaifallah, H. Rezk, M. Ahmed, Optimal design and economic analysis of a hybrid renewable energy system for powering and desalinating seawater, Energy Reports 9 (2023) 2473–2493. https://doi.org/10.1016/j.egyr.2023.01.087.

[12] U. Caldera, D. Bogdanov, S. Afanasyeva, C. Breyer, Role of Seawater Desalination in the Management of an Integrated Water and 100% Renewable Energy Based Power Sector in Saudi Arabia, Water 10 (2017) 3. https://doi.org/10.3390/w10010003.

[13] N.S. Hassan, A.A. Jalil, S. Rajendran, N.F. Khusnun, M.B. Bahari, A. Johari, M.J. Kamaruddin, M. Ismail, Recent review and evaluation of green hydrogen production via water electrolysis for a sustainable and clean energy society, International Journal of Hydrogen Energy 52 (2024) 420–441. https://doi.org/10.1016/j.ijhydene.2023.09.068.

[14] S.N. Ababneh, M. Al-Odat, Optimal Design of a Hybrid Renewable Power System for a Reverse Osmosis Desalination Plant in Jordan, J. Ecol. Eng. 25 (2024) 384–397. https://doi.org/10.12911/22998993/188917.

[15] P. Cabrera, J.A. Carta, C. Matos, E. Rosales-Asensio, H. Lund, Reduced desalination carbon footprint on islands with weak electricity grids. The case of Gran Canaria, Applied Energy 358 (2024) 122564. https://doi.org/10.1016/j.apenergy.2023.122564.

[16] E. Najjar, M. Al-Hindi, M. Massoud, W. Saad, Life cycle assessment and cost of a seawater reverse osmosis plant operated with different energy sources, Energy Conversion and Management 268 (2022) 115964. https://doi.org/10.1016/j.enconman.2022.115964.

[17] S. Schär, A. Bischi, A. Baccioli, U. Desideri, J. Geldermann, Optimization of sustainable seawater desalination: Modeling renewable energy integration and energy storage concepts, Energy Conversion and Management 293 (2023) 117447. https://doi.org/10.1016/j.enconman.2023.117447.

[18] R. d'Amore-Domenech, Ó. Santiago, T.J. Leo, Multicriteria analysis of seawater electrolysis technologies for green hydrogen production at sea, Renewable and Sustainable Energy Reviews 133 (2020) 110166. https://doi.org/10.1016/j.rser.2020.110166.

[19] J. Mustafa, S. Alqaed, F.A. Almehmadi, E.H. Malekshah, M. Sharifpur, Effect of economic and environmental parameters on multi-generation of electricity, water, heat, and hydrogen in Saudi Arabia: A case study, International Journal of Hydrogen Energy 52 (2024) 585–598. https://doi.org/10.1016/j.ijhydene.2023.07.035.

[20] S. Rehman, K.M. Kotb, M.E. Zayed, A.S. Menesy, K. Irshad, A.S. Alzahrani, A.A. Al-Shaikhih, M. Mohandes, Wind to Hydrogen: A Case Study in Aqaba Gulf, in: 2024 6th International Symposium on Advanced Electrical and Communication Technologies (ISAECT), IEEE, 2024: pp. 1–6. https://doi.org/10.1109/isaect64333.2024.10799578.

[21] H. Rezk, M. Alghassab, H.A. Ziedan, An Optimal Sizing of Stand-Alone Hybrid PV-Fuel Cell-Battery to Desalinate Seawater at Saudi NEOM City, Processes 8 (2020) 382. https://doi.org/10.3390/pr8040382.

[22] K. Taroual, M. Nachtane, M. Rouway, M. Tarfaoui, A. Faik, V. Mînzu, K. Hilmi, D. Saifaoui, Marine Renewable-Driven Green Hydrogen Production toward a Sustainable Solution and a Low-Carbon Future in Morocco, JMSE 12 (2024) 774. https://doi.org/10.3390/jmse12050774.

[23] H. Barghash, A. Al Farsi, K.E. Okedu, B.M. Al-Wahaibi, Cost benefit analysis for green hydrogen production from treated effluent: The case study of Oman, Front. Bioeng. Biotechnol. 10 (2022). https://doi.org/10.3389/fbioe.2022.1046556.

[24] P. Woods, H. Bustamante, K.-F. Aguey-Zinsou, The hydrogen economy - Where is the water?, Energy Nexus 7 (2022) 100123. https://doi.org/10.1016/j.nexus.2022.100123.

[25] M. León, J. Silva, R. Ortíz-Soto, S. Carrasco, A Techno-Economic Study for Off-Grid Green Hydrogen Production Plants: The Case of Chile, Energies 16 (2023) 5327. https://doi.org/10.3390/en16145327.

[26] A. Badruzzaman, S. Karagoz, F. Eljack, Sustainable-green hydrogen production through integrating electrolysis, water treatment and solar energy, Front. Chem. Eng. 7 (2025). https://doi.org/10.3389/fceng.2025.1526331.

[27] M.K. Hassan, H. Rezk, H. Youssef, A.S. Shehata, A.A. El-Bary, A. Al-Quraan, Optimal Sizing and Management of Hybrid Wind Turbine-Diesel-Battery System for Reverse Osmosis Seawater Desalination in NEOM City, International Journal of Energy Research 2024 (2024). https://doi.org/10.1155/2024/2941404.

Рамазан А. Қ., Тайжанова Л.С., Сырлыбекқызы С.

БАТЫС ҚАЗАҚСТАНҒА АРНАЛҒАН ГИБРИДТІ ЖАҢАРТЫЛАТЫН ЭНЕРГИЯМЕН ЖҰМЫС ІСТЕЙТІН ТӨМЕН КӨМІРТЕКТІ КЕРІ ОСМОС ТҰЩЫЛАНДЫРУ ЖҮЙЕСІН ЭКОЛОГИЯЛЫҚ БАҒАЛАУ

Аңдатпа. Климаттың өзгеруі мен жедел экономикалық өсудің әсерінен күшейген жаһандық су тапшылығы теңіз суын кері осмос арқылы тұщыландыруға (SWRO) тәуелділіктің артуына алып келді. Қазіргі таңда SWRO әлемдік тұщыландыру қуаттылығының 70 %-дан астамын құрағанымен, бұл процесс энергияны көп қажет етеді және әдетте бір текше метр суға 3–5 кВт·сағ электр энергиясын тұтынады. Қазба отын негізіндегі электр энергиясын пайдалану тұщыландырудың экологиялық артықшылықтарын әлсіретіп, климаттық міндеттемелерге қайшы келеді. Осы зерттеуде Батыс Қазақстанның құрғақ аймағындағы тәулігіне 100 м³ өнімділігі бар SWRO қондырғысы үшін төмен көміртекті гибридті энергетикалық жүйенің техника-экономикалық және экологиялық көрсеткіштері талданады. Сағаттық жел деректері мен HOMER Pro модельдеуі негізінде үш дана 95 кВт жел турбинасынан, 25 кВт дизель генераторынан, 1,2 МВт·сағ литий-ион аккумуляторлық батареялар блогынан және 20 кВт түрлендіргіштен тұратын оңтайлы конфигурация анықталды. Нәтижелер оңтайландырылған жүйенің тек дизельге негізделген базалық нұсқамен салыстырғанда айтарлықтай артықшылыққа ие екенін көрсетті: таза дисконтталған шығын $7,11 млн-нан $2,06 млн-ға дейін төмендеді, ал электр энергиясының теңестірілген құны (LCOE) 0,5907 USD·кВт·сағ$^{-1}$ болды. Жел энергиясы жылдық жүктеменің 84,8 %-ын қамтамасыз етіп, дизель тұтынуын 12 770 литрге дейін азайтты және CO_2 шығарындыларын жылына шамамен 63 тоннаға қысқартты. Алайда жел қуатының

артық таңдалуына байланысты өндірілген электр энергиясының шамамен 84 %-ы пайдаланылмай шектеледі, бұл озық гибридті жүйелермен салыстырғанда LCOE деңгейінің жоғары болуына әкеледі. Зерттеу жел-дизель-аккумулятор жүйелері Батыс Қазақстан жағдайында сенімді әрі төмен көміртекті сумен жабдықтауды қамтамасыз ете алатынын көрсетеді. Дегенмен артық өндірісті азайту, экономикалық тиімділікті арттыру және тұрақтылықты күшейту үшін фотоэлектр генерациясын біріктіру, артық электр энергиясын сату немесе жасыл сутегі өндіруді енгізу маңызды.

Кілт сөздер: теңіз суын кері осмос арқылы тұщыландыру; төмен көміртекті технология; жел-аккумулятор жүйесі; электр энергиясының теңестірілген құны; HOMER Pro; Батыс Қазақстан; жасыл сутегі; су-энергия байланысы.

Рамазан А. Қ., Тайжанова Л.С., Сырлыбекқызы С.

ЭКОЛОГИЧЕСКАЯ ОЦЕНКА НИЗКОУГЛЕРОДНОГО ОБРАТНОГО ОСМОСА МОРСКОЙ ВОДЫ С ИСПОЛЬЗОВАНИЕМ ГИБРИДНЫХ ВОЗОБНОВЛЯЕМЫХ ИСТОЧНИКОВ ЭНЕРГИИ ДЛЯ ОПТИМИЗАЦИИ В ЗАПАДНОМ КАЗАХСТАНЕ

Аннотация. Глобальная нехватка воды, усугублённая изменением климата и быстрым экономическим ростом, привела к росту зависимости от опреснения морской воды методом обратного осмоса (SWRO). Хотя на SWRO приходится более 70 % мировой мощности опреснения, этот процесс остаётся энергоёмким и обычно потребляет 3–5 кВт·ч на м³. Использование электроэнергии на основе ископаемого топлива подрывает экологические преимущества опреснения и противоречит климатическим обязательствам. В настоящем исследовании анализируются технико-экономические и экологические характеристики низкоуглеродной гибридной энергетической системы для установки SWRO производительностью 100 $м^3 \cdot сут^{-1}$ в засушливом регионе западного Казахстана. Для оценки использованы почасовые данные ветра и моделирование в HOMER Pro с целью определения оптимальной конфигурации трёх ветряных турбин по 95 кВт, дизель-генератора 25 кВт, батареи на 1,2 МВт·ч и преобразователя 20 кВт. Результаты показывают, что оптимизированная система существенно превосходит базовую схему только на дизеле: чистая приведённая стоимость (Net Present Cost, NPC) снижается с $7,11 млн до $2,06 млн, а приведённая стоимость электроэнергии (LCOE) снижается до 0,5907 $USD \cdot кВт \cdot ч^{-1}$. Ветровая энергия обеспечивает 84,8 % годовой нагрузки, сокращая потребление дизеля до 12 770 литров и уменьшая выбросы CO_2 примерно на 63 $т \cdot год^{-1}$. Вместе с тем примерно 84 % вырабатываемой электроэнергии оказывается невостребованной (curtailment) из-за избыточной установленной ветровой мощности, что приводит к относительно высокой приведённой стоимости по сравнению с передовыми гибридными системами. Исследование делает вывод, что ветро-дизель-аккумуляторные системы способны обеспечить надёжное низкоуглеродное водоснабжение в западном Казахстане, однако интеграция фотоэлектрической генерации, реализация избыточной электроэнергии либо производство «зелёного» водорода необходимы для минимизации сбросов, повышения экономической целесообразности и улучшения устойчивости.

Ключевые слова: опреснение морской воды; низкоуглеродная технология; ветро-аккумуляторная система; приведённая стоимость электроэнергии (LCOE); HOMER Pro; Западный Казахстан; зелёный водород; взаимосвязь вода — энергия.